Heat Transfer in the Critical Region—Temperature and Velocity Profiles in Turbulent Flow

RODNEY D. WOOD and J. M. SMITH

Northwestern University, Evanston, Illinois

Unusual heat transfer phenomena have been observed between solid surfaces and fluids near their thermodynamic critical point. To understand better these phenomena temperature and velocity profiles and local heat transfer coefficients were measured for turbulent flow of carbon dioxide in a tube at 1,075 lb/sq. in. abs. (p_c = 1,071). The results indicate a severe flattening of the radial temperature profiles, a maximum in the velocity profile between the wall and the tube axis, and a maximum in h' when the bulk fluid temperature passes through the transposed critical temperature.

The results can be explained qualitatively by considering the variation with temperature of thermal conductivity near the tube wall and specific heat in the turbulent core.

Heat transfer from a solid surface to a fluid near its critical temperature and pressure has been studied for the past decade (*2, 4, 5, 6, 7, 8, 11, 12, 14*). In the immediate region of the critical point the experimental studies (*6, 7, 11, 14*) indicate unusual heat transfer coefficients which have not been satisfactorily explained. Of particular interest is the maximum observed in h' (the prime designates the local or point values of h) when the fluid is heated at its critical pressure from below to above the critical temperature. The situation is made more difficult because the fluid properties, especially thermal conductivity, are subject to some uncertainty in the critical region. Understanding of the problem would be improved if the behavior of the fluid near the heated surface were known. Therefore an investigation has been made of temperature and velocity profiles for carbon dioxide in turbulent flow in a tube at 1,075 lb./sq.in.abs. (critical pressure = 1,071 lb./sq.in.abs.). Heat transfer rates were measured so that the transfer coefficients corresponding to the profiles were also known.

APPARATUS

The essential part of the apparatus was an Inconel tube, used as a resistance heater, through which the carbon dioxide flowed. With the resistance heater the local heat input was known, and a point heat transfer coefficient could be calculated. This was necessary in order to obtain h' at the axial position where the profiles were measured. A schematic diagram of the equipment is given in Figure 1. The test section was an Inconel tube, seamless, cold drawn, and annealed. Inconel was selected for its very small temperature coefficient of resistivity (about 7×10^{-5} °F.$^{-1}$). The outside diameter was 1.000 in., the inside diameter 0.902 in., and the total length of the tube was 56½ in. Two electrical terminal bars were fashioned of ½-in. copper plate; they were drilled and reamed to fit over the tube and were soldered in place. The actual heated section was 30.1 in. long, measured inside the terminal bars. The 21-in. length of the tube upstream from the heated section (Figure 1) served to give a close approach to a fully developed velocity profile. The location at which the profiles were measured was 27.7 in. from the beginning of the heated section. Several investigators (*1, 3, 10*) have found the thermal entrance length-to-diameter ratio to be less than this. This was confirmed by the fact that at the profile location the temperature at the center of the tube was always higher than the bulk temperature at the entrance to the test section. For wall temperature measurements thirteen copper-constantan thermocouples were soldered to the outer wall at various axial locations. The test section was mounted vertically and covered with 2½-in. of insulation.

The traverse device for profile measurements is shown in Figure 2. The upper end chamber was a block of steel machined as shown. A rod of stainless steel passed through the block and was free to move back and forth. The probe was inserted through a reamed hole in the traverse rod, seated in a recess, and screwed in place. The position of the rod was controlled by a hand-nut bearing on a heavy plate. The nut was scribed in divisions corresponding to 0.001 in., and the probe could be positioned at least that accurately. The reading of the nut when the probe touched the wall was determined as follows. The test section was insulated from the rest of the equipment. Then a circuit was set up with a vacuum tube voltmeter and arranged so that the circuit was completed when the probe tip touched the wall. The measurements were repeatedly checked with flow in the test section, and it was found that the position could always be reproduced within 0.001 in. For both temperature and velocity profiles

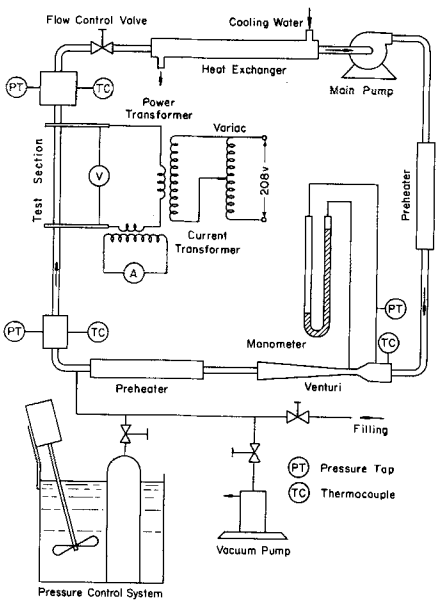

Fig. 1. Schematic diagram of equipment.

Rodney D. Wood is at the University of Nebraska, Lincoln, Nebraska; J. M. Smith is at the University of California, Davis, California.

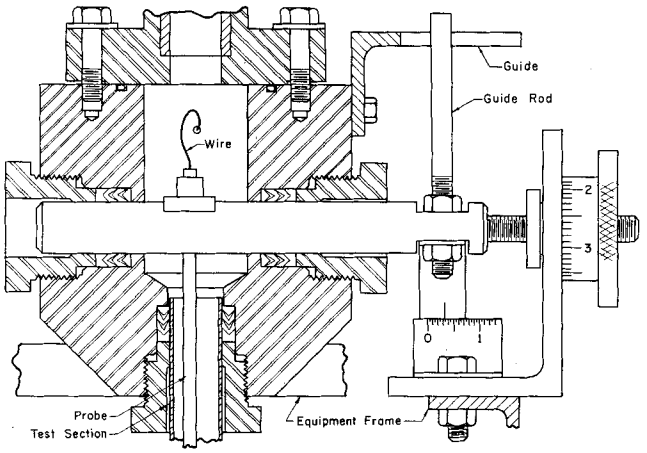

Fig. 2. Upper end chamber and traverse device.

fifteen positions were used across the radius of the tube. The closest measurement to the wall was at a radial position y/r of 0.022, or approximately 0.01 in. from the wall. For the traverse rod a packing was required which would give pressure sealing and yet permit movement. Also it was necessary to insulate the test section electrically from the rest of the plumbing. Chemlon style CV-H rings were used for both purposes.

The probes were made of ¼-in. stainless steel high pressure tubing. The temperature probe was made by nosing down to ⅛-in. tubing, then to 0.050 tubing. The very tip of the probe was the bead of a copper-constantan thermocouple, of 36 gauge wire. This bead was honed until it was about 0.007 in. thick in a direction along a radius of the tube.

The velocity probe had two tips. Each was made of No. 16 (0.060 in.) hypodermic tubing. The impact tube was made by flattening the end of the tube. A shim of 0.006-in. spring steel was used to obtain a slit of regular shape. After flattening the tube was bent to produce the necessary offset and then honed to reduce the outside wall thickness to 0.004 in. The static tube was made by cross drilling two 0.018-in. holes, making four holes in all, and fitting the end with a nose.

Each probe extended 8½ in. below the bottom of the traverse rod. Details about the probes are given in reference 22.

Measurement

Pressure taps at three points in the flow scheme, the Venturi, test section inlet, and test section outlet were connected to a manifold which in turn was connected to a Heise bourdon tube pressure gauge. The gauge had a range of 1,500 lb./sq.in. and was graduated in divisions of 1 lb./sq.in. Thermocouples to measure bulk temperature were installed at the same three locations. These were copper-constantan, 30 gauge, with exposed beads. A mixing chamber was used at the outlet of the test section to ensure measurement of a bulk mean temperature. These three thermocouples were calibrated with a hypsometer and were then used to calibrate the thirteen couples on the wall of the test section and the one on the probe, in place. Measurement of thermocouple electromotive force was done with a portable potentiometer which could be read to 1 mv.

An inclined manometer was used in conjunction with the velocity probe to obtain measurements of dynamic head. The manometer was mounted on a tilting bed to allow variation of the inclination; the angle to the horizontal could be read to the nearest half minute.

Flow rates were measured with a Venturi meter (Figure 1) calibrated with water. The heat transfer rate was determined by measuring the electrical power input with a 0 to 5 amp a.c. ammeter and a 0 to 15/0 to 30 v. a.c. voltmeter. Complete details of the apparatus are given elsewhere (22).

The pitot tube was calibrated by comparing the total flow rate obtained from the measured profile with the flow rate indicated by the Venturi meter. The results for the four calibration runs, all with carbon dioxide at 1,075 lb./sq.in.abs.; are as follows:

Temperature, °F.	Density, lb./cu.ft.	Flow rate—lb./sec. Venturi	Pitot tube profile
79.5	46.2	2.62	2.63
83.4	43.3	2.48	2.45
88.0	34.0	1.57	1.57
85.0	41.6	1.65	1.66

In addition to the overall agreement noted above experimental profiles were compared with those calculated from the universal velocity distribution equations (*16*). For example for one run at a Reynolds number of 1.11×10^6 the average deviation of measurements at sixteen radial positions from calculated valves at the same radial positions was less than 0.3%. This agreement indicates that the probes did not significantly affect the flow while measurements were made, and that while temperature and velocity data were obtained on separate runs the reproducibility was such that measurements from two separate runs could be used as though it originated from one run.

The carbon dioxide was of 99.9% purity.

Operation

Conditions for the series of runs at various bulk temperatures were obtained as follows. At the lowest temperature of the series a convenient flow rate was set. The flow control valve was not changed thereafter during the series. This resulted in the mean test section velocity being nearly the same for all runs in the series, even though mass flow rates dropped steadily with increasing temperature. Temperature profiles were taken at specific inlet temperatures, all at the same heat flux and all with the same exit pressure. Exit pressure was used instead of inlet pressure because it was much closer to the location of the probe.

Four runs were also taken with one flow rate, one pressure, and one temperature at the center of the tube for different values of heat flux.

The apparatus was then partially dismantled, and the necessary changes were made to measure velocity profiles. Each velocity profile recorded was taken under conditions of inlet temperature, exit pressure, heat flux, and flow rate duplicating those for the corresponding temperature profiles. The range of variables investigated is given in another section.

PROPERTIES IN THE CRITICAL REGION

The accepted values for the critical point properties of carbon dioxide are (*20*)

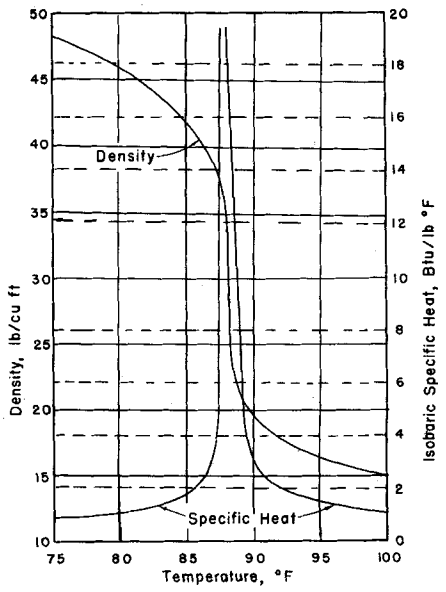

Fig. 3. Specific heat and density of carbon dioxide at 1,075 lb./sq.in.abs.

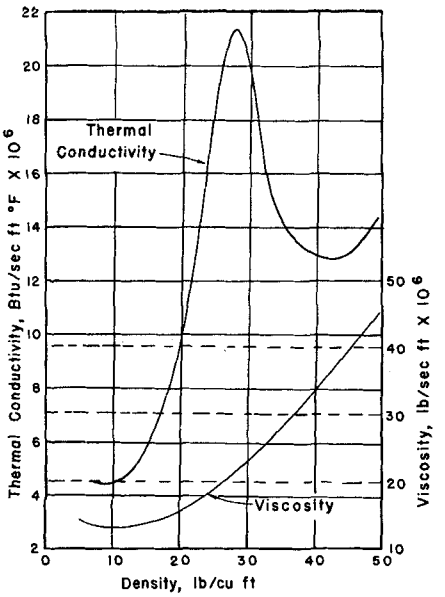

Fig. 4. Thermal conductivity and viscosity of carbon dioxide at 1,075 lb./sq.in.abs.

$t_c = 87.8°F.$

$p_c = 1{,}071$ lb./sq.in.abs.

$\rho_c = 29.0$ lb./cu.ft.

The transposed critical temperature t_c', defined as the temperature for which the specific heat is a maximum, is 88.1°F. at 1,075 lb./sq.in.abs. and 89.0°F. at 1,100 lb./sq.in.abs. (*15*).

Figure 3 shows the variation of density and heat capacity with temperature at 1,075 lb./sq.in.abs. The data used to plot the curve for density were taken from several sources, chiefly Michels et al. (*17, 18*) and Jenkin (*13*). The heat capacity curve is based upon the data of Koppel and Smith (*15*).

The viscosity and thermal conductivity at the same pressure are shown in Figure 4. There is considerable disagreement over the behavior of these quantities in the critical region, but the curves given here are believed to represent the most credible data. Values of viscosity were obtained from several sources, the most important being Naldrett and Maass *(19)*. The curve for thermal conductivity is based on the data of Sengers and Michels (*21*) and Guildner (*9*). A complete analysis of the transport property information available as well as other data is given in reference *22*.

EXPERIMENTAL RESULTS

Data were taken to examine the effect of bulk temperature and heat flux on temperature profiles, velocity profiles, and heat transfer coefficient. For convenience in discussion the results will be grouped according to effect. However at first it is desirable to present some general observations about the data.

General Comments on Experimental Measurements

Heat Balances. An energy balance could be evaluated from the measured power input, flow rate, and bulk temperature, and the heat capacity. The latter information was available from Koppel's enthalpy data (*15*). For runs where the bulk temperature was well below the transposed critical temperature (up to 72°F.) the agreement between the electrical heat input and energy added to the fluid was within 2%. At temperatures close to t_c' deviations up to 20% were common. There were two reasons for this. First at temperatures near t_c' the specific heat is so large that the difference between inlet and outlet bulk temperatures becomes less than 1.0°F. For example for run No. 27 these temperatures were 86.0 and 86.4°F. Since the measuring equipment was sensitive to about 0.03°F., the temperature difference may be in error by 15%. Second the pressure drop due to hydrostatic head and friction in the vertical test section reached significant values, for example 3.0 lb./sq.in.abs. for run No. 27. In the critical region the Joule-Thomson coefficient is so large that this pressure difference could cause an isenthalphic temperature change of more than 0.1°F. Because of these effects bulk mean temperatures at the probe location were evaluated from the measured temperatures at the inlet and outlet of the test location rather than from an energy balance.

Heat loss calculations indicated a maximum loss from the insulated surface of 0.3%.

Fluctuations and Control. When measurements were taken within about 1°F. of t_c', temperature fluctuations made it difficult to get representative values. The changes appeared to be sudden, almost step changes, and their frequency varied from one half to one or more seconds. The magnitude increased near the wall; t_w values varied up to 2.0°F., while at $y/R = 0.05$ the range was about 1.0°F. Similar fluctuations in velocities for data near t_c' were not observed. Associated with the temperature fluctuations were difficulties in controlling preassigned operating conditions. For example near the transposed critical temperature a change of 0.1°F. in inlet fluid temperature introduced a change of 0.3°F. at the profile measurement location and $y/R = 0.5$.

Finally it should be mentioned that the agreement was poor between flow rates from the Venturi meter and integrated velocity profiles for runs where the density is changing most rapidly, that is when the temperature profile included the transposed critical temperature. It will be noted that the tabular data presented earlier to substantiate the pitot calibration corresponded to bulk mean temperatures below t_c'.

The Effect of Bulk Temperature

A series of temperature profiles, for various bulk temperatures, were taken at 1,075 lb./sq.in.abs. These runs were made at the same heat flux, 37,200 B.t.u./hr.(sq.ft.), and approximately the same average velocity at the test location, 13.5 ft./sec. The Reynolds numbers vary somewhat, owing to the irregular property variations. These profiles are shown in Figure 5. At temperatures well below t_c' the shape of the profile is fairly similar to the shape expected for a fluid with constant properties. As the bulk temperature is increased, the profile gradually becomes flattened, and as t_c' is approached, it becomes exceedingly flat. There is then a rapid change to a more rounded profile as the bulk temperature is raised above the transposed critical. Runs 29 and 30 cover the significant region where the bulk temperature is on either side of t_c'.

Another series (twenty runs) of temperature profiles were made at 1,100 lb./sq.in.abs. They showed the same effect as the data in Figure 5.

Velocity profiles were obtained for operating conditions matching those of the temperature profiles taken at 1,075 lb./sq.in.abs. The pitot tube gives readings of local dynamic head ρv^2, and it is necessary to have values of local density in order to calculate the local velocity. Densities were obtained from the measured temperature profiles and the plot of density vs. temperature shown in Figure 3. For Runs 22 through 28 values of density were used directly as they were given by the profiles and chart. For Runs 29 and 30 the temperature profiles encompassed the region of high density gradient and subjected the de-

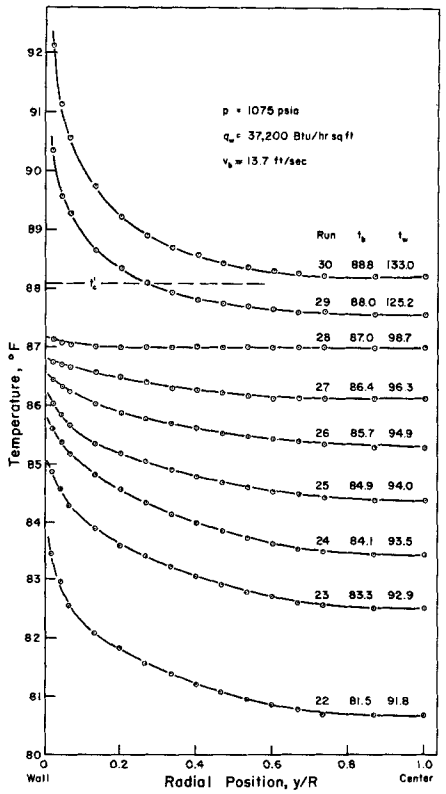

Fig. 5. Effect of bulk temperature on temperature profiles.

termination of local density to considerable error. Accordingly for these two runs the densities taken from the chart were first used to construct a graph of density vs. radial position. Values taken from this smoothed plot were then used to compute velocities.

The results of Runs 22 through 28 are given in Figure 6. Run 28 gave data lower than that for the other six, but

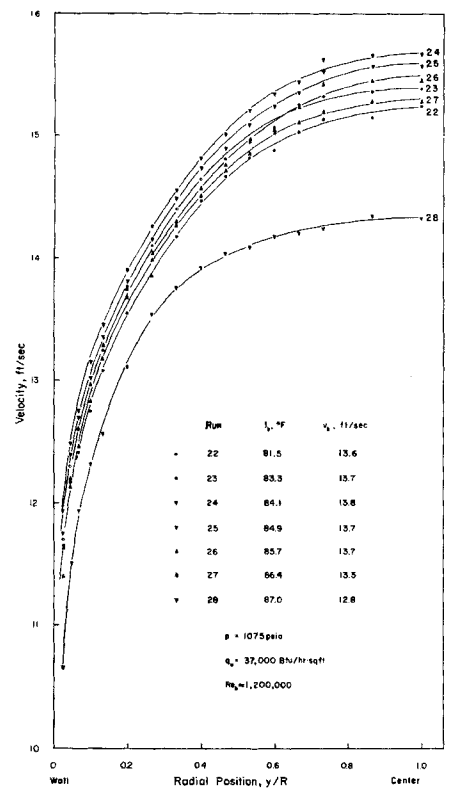

Fig. 6. Velocity profiles.

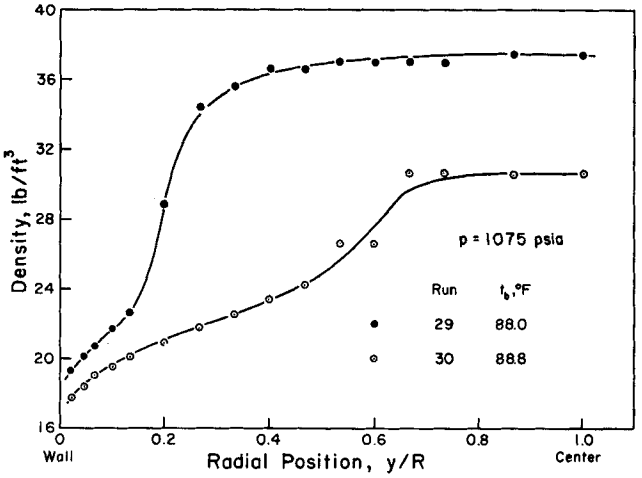

Fig. 7. Density profiles, based on temperature profiles.

this is believed due to equipment characteristics and the method of choosing operating conditions. The density profiles for Runs 29 and 30 are given in Figure 7, and Figure 8 shows the velocity profiles for these two runs. It is important to note that the unusual shapes of these profiles are consequences of the density profiles and not of the measurements of dynamic head. There is nothing in the pitot tube measurements that suggests such behavior. A careful check was made of the pitot tube readings, and it was concluded that these were not in error.

Outer wall temperatures and heat flux were measured for all runs. The outer wall values were converted to inner wall temperatures t_w from the known heat flux and thermal conductivity of Inconel. Then heat transfer coefficients were computed in accordance with the equation

$$h' = \frac{q_w}{t_w - t_b} \qquad (1)$$

The effect of bulk temperature on h' is shown in Figure 9. (The data from the 1,100 lb./sq.in.abs. runs are included here.) At temperatures well below t'_c, h' increases with temperature, and as the bulk temperature approaches t'_c the increase is rapid. A maximum is reached just below t'_c, and with a further increase in temperature h' decreases very sharply. It appears that the maximum rate of decrease occurs when the bulk temperature is equal to the transposed critical temperature.

The Effect of Heat Flux

Four runs were taken, as follows:

Pressure:	1,075 lb./sq.in.abs.
Bulk Reynolds number:	930,000

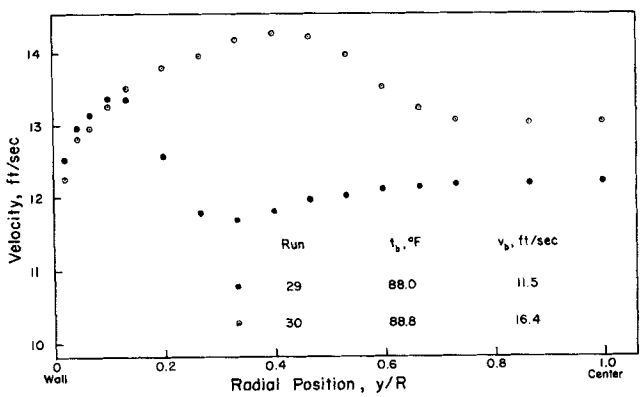

Fig. 8. Velocity profiles.

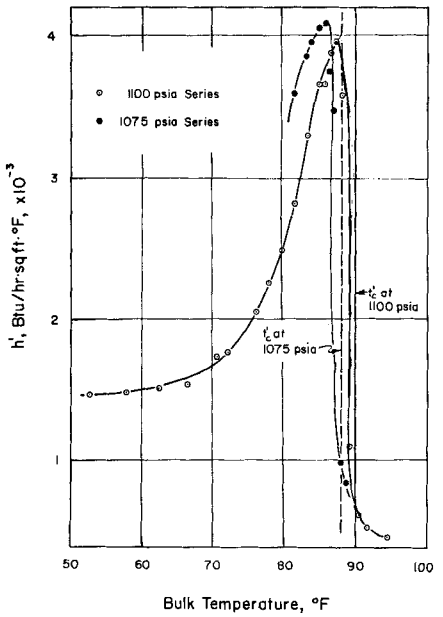

Fig. 9. Effect of bulk temperature on heat transfer coefficient.

Temperature at the center of the tube: 85°F.

Heat flux: Run 34 65,000 B.t.u./hr. (sq.ft.)
35 40,000
36 20,000
37 10,300

The Reynolds numbers actually ranged from 910,000 to 950,000, owing to the fact that the bulk temperature varied slightly (it was chosen to keep the center temperature constant). Wall and bulk temperatures were

Run	t_b, °F.	t_w, °F.
34	86.0	129.6
35	85.6	102.6
36	85.4	90.7
37	85.1	87.6

As the heat flux is increased, both profiles become relatively flatter. The effect on the temperature profile is shown in Figure 10, which compares dimensionless profiles for Runs 34 and 36. Figure 11 shows the dimensionless velocity profiles. Deissler has predicted this flattening,

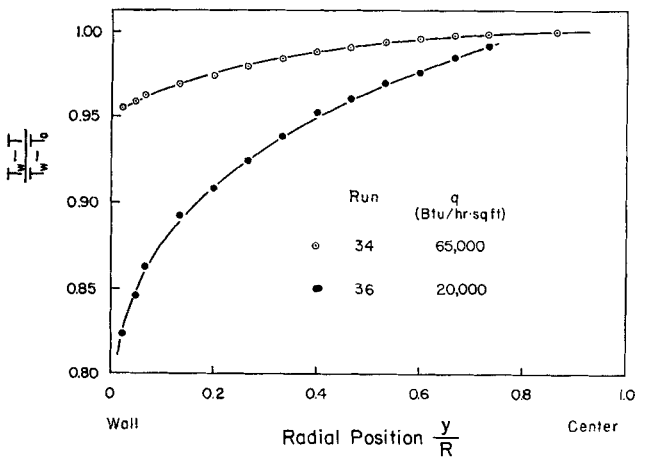

Fig. 10. Effect of heat flux on temperature profiles.

stating that it might not be possible to verify it experimentally (*4, 5*).

It is well to point out that the density gradients for these runs were not large, as they were for the unusual velocity profiles reported earlier (Runs 29 and 30). While it is true that these profiles, like the others, were computed and not directly measured, the values of density used in these four runs are subject to much less error than those used for Runs 29 and 30.

The values of heat transfer coefficient for these four runs are

Run	q_w, B.t.u./hr. (sq. ft.)	h', B.t.u./hr. (sq. ft. °F.)
34	65,000	1460
35	40,000	2360
36	20,000	3780
37	10,300	4140

Heat flux is seen to have a considerable effect on the heat transfer coefficient. It is possible to express this same information as the effect of wall temperature on h'. This will be discussed later.

DISCUSSION OF RESULTS

Unusual Velocity Profiles

In considering the unusual profiles for Runs 29 and 30 (Figure 8) four possibilities for error must be examined: the temperature profiles are incorrect, the pVT data are incorrect, equilibrium pVT behavior does not hold at high Reynolds number with heat transfer, and the measurements of dynamic head are incorrect. The consistency of the measurements makes the first and last seem unlikely. Local disequilibrium is generally considered to exist only in such phenomena as shocks, and this rules out the third. The second possibility is more promising. However the temperature at which the density changes most rapidly cannot be in error by more than about 0.1°F., and some profile will certainly include this temperature. Density profiles with large gradients far from the wall would therefore still be drawn. Hence this possibility affords grounds for dissent only on the particular shape of the unusual profiles and not on the fact of their occurrence.

Under appropriate conditions profiles as shown in Figure 8 are entirely plausible for laminar flow, and there seems to be no fundamental objection to them in turbulent flow. The analysis by Hsu and Smith (*12*) indicated that for $(N_{Gr})/(r^+)^3$ greater than about 0.01 the velocity profile would be greatly affected and that the maximum velocity would not be at the center of the tube if the bulk density were sufficiently large. For Run 29 $(N_{Gr})/(r^+)^3$ was estimated to be only 0.001. However the profiles of Hsu and Smith were calculated for a pressure of 1,200 lb./sq. in. abs., and a value of the dimensionless heat flux parameter β of 0.0015. For Run 29 β was 0.009 and the pressure was 1,075, much closer to the critical pressure. It is not unreasonable that these differences account for the matter. Finally the four runs taken at various heat fluxes showed that the velocity profile was affected even when density gradients were quite moderate. It is therefore concluded that velocity profiles with maxima at positions other than the center, as shown in Figure 8, do exist.

Heat Transfer Coefficients

As shown in Figure 9 a plot of h' vs. bulk temperature (for constant heat flux) reveals a pronounced maximum at or just below the transposed critical temperature. If these same heat transfer coefficients are plotted against wall temperatures, there is a very sharp peak at about

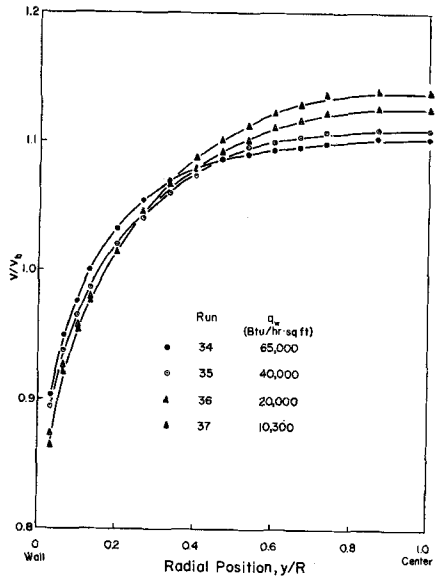

Fig. 11. Dimensionless velocity profiles.

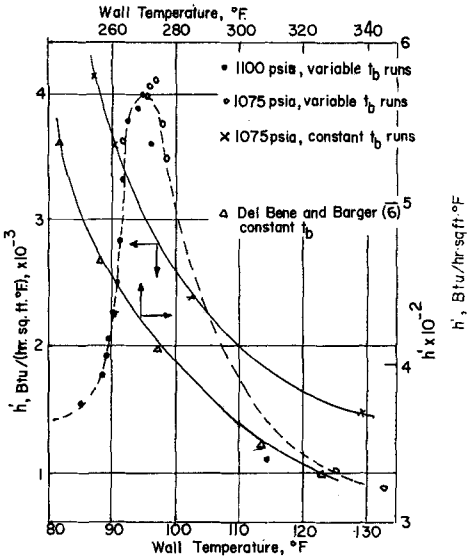

Fig. 12. Effect of wall temperature on heat transfer coefficient.

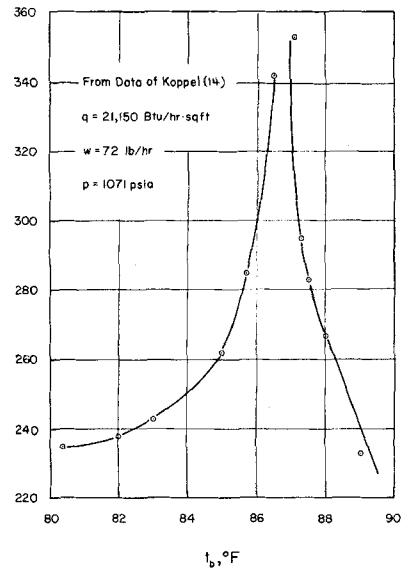

Fig. 13. Effect of bulk temperature on heat transfer coefficient.

96°F. dotted line (Figure 12.). This is the phenomenon reported by Dickinson and Welch (7) for water and by Del Bene and Barger (6) for Freon-12. However the four runs taken at various heat fluxes and essentially a single bulk temperature (upper solid line) show that the peak is not caused by the wall temperature. The wall temperatures for these runs bracket the peak temperature, and h' decreases smoothly.

To support this point data were taken from Del Bene and Barger to form a plot of h' vs. wall temperature for a single bulk temperature, and this is shown as the lower curve in Figure 13. The data correspond to the following conditions:

Flow rate:	790 lb./hr.
Pressure:	600 lb./sq. in. abs.
Bulk temperature:	215°F.
Heat flux:	15,000 to 37,000 B.t.u./hr. (sq. ft.)

For Freon — 12, $P_c = 596$ lb./sq. in. abs.
$t_c = 233.6$°F.

This lower curve is similar to the upper curves for the present data showing that h' decreased continuously with increasing t_w.

The data of Dickinson and Welch do not include enough values for one bulk temperature and one flow rate to form a plot of this sort, but inspection of their tables reveals that low wall temperatures generally occurred for bulk temperatures below t'_c, and high values of t_w were found for t_b above t'_c. It is therefore suspected that their peak was due to bulk temperature.

Bulk temperature has been considered by previous investigators. Koppel (14) took enough data at one flow rate and one heat flux to permit a graph of h' vs. t_b to be drawn, and this is given in Figure 13. The appearance of a sharp maximum in h' just below the transposed critical temperature agrees well with the findings of this study (Figure 9).

From the available data it is concluded that the maximum in the heat transfer coefficient is properly associated with the fluid bulk temperature and not the wall temperature.

Explanation of Phenomena

Next to the tube wall the dominant mechanism for heat transfer is conduction and the significant property should be the thermal conductivity. In the turbulent core the significant variable should be the heat capacity, or the product of heat capacity and density.

Suppose k'_w is an average thermal conductivity for the region very close to the wall. A rigorous definition is not necessary, but it may be said that the region corresponds approximately to the thickness of the laminar sublayer. For an average heat capacity for the core take the value at the bulk temperature. Recall that for C_p there is a sharp maximum at t'_c and that the thermal conductivity generally decreases with temperature but shows a sudden peak somewhere near t'_c (see Figures 3 and 4). In terms of this oversimplified model of a laminar layer and a turbulent core the variations of k'_w and C_{pb} with temperature can be shown to account for the observed phenomena.

The flattening of the temperature profile as the bulk temperature is increased up to t'_c, and the subsequent rapid change back to a rounded shape (*Figure* 5). As t'_c is approached, C_{pb} is large and rapidly becoming larger. Heat transfer due to mixing is improved, and the temperature gradients in the core are lowered. The flattening is aided by the fact that below t'_c, C_p increases with temperature so that turbulent heat transport is better moderately close to the wall than near the center.

Once above t'_c the reverse holds. C_{pb} is still large, and the profile is still relatively flatter than it was at a low temperature. However because C_p decreases with temperature above t'_c, the turbulent energy transport is worse near the wall than near the center, and consequently the temperature gradient exhibits a more rapid increase closer to the wall.

The behavior of h' with bulk temperature. This is best understood by considering how conditions affect the wall temperature for a situation in which the heat flux is fixed. As the bulk temperature is increased, and the wall temperature goes above t'_c, the average k'_w increases greatly, owing to the peak in thermal conductivity. There is improved heat transfer in the core, which is in effect an excellent heat sink because of the very large C_{pb}. Both of these factors tend to prevent the wall temperature from increasing. Therefore the heat transfer coefficient is large. Once the bulk temperature is above t'_c, k'_w takes a sharp drop, core resistance increases, and the wall temperature is abruptly raised. Consequently the decrease in h' above t'_c *is* much more rapid than the increase below.

From the foregoing discussion it seems that the derivative of C_p, whether C_p increases or decreases with temperature, may be as important as its magnitude.

The effect of heat flux on the temperature profile. As the heat flux is increased, the temperature at the edge of the core is raised. The increase in C_p leads to better turbulent heat transport. Although the temperature gradients in the core increase, they do not increase in proportion to the heat flux, Therefore the profiles become relatively flatter as the flux is increased.

The effect of heat flux on the heat transfer coefficient. With increased heat flux the wall temperature increases and k'_w is lowered. These are mutually aggravating events. Consequently the resistance of the sublayer becomes large and h' decreases. Reference to the solid lines in Figure 12 indicate that the curves are approximately described by

$$h' \sim \frac{1}{t_w - t'_c} \qquad (2)$$

This is in agreement with the model; that is the decrease in h' should be most rapid at a wall temperature near the transposed critical value.

The effect of heat flux on the velocity profile supports this reasoning. In the core the density and viscosity are nearly the same for the different heat fluxes. In the sublayer as the heat flux increases the temperature increases, and the velocity decreases. The result should be a higher velocity gradient in the sublayer and a lower one in the core. The profiles in Figure 11 do show this variation with heat flux.

CONCLUSION

The significant findings of this study may be summarized as follows.

1. The temperature profiles flatten significantly when the bulk mean temperature passes through the transposed critical temperature.
2. Velocity profiles show unusual behavior with possible maxima at a radial position away from the center of the tube.
3. The sharp peak in heat transfer coefficient is actually associated with bulk temperature not wall temperature. At constant bulk temperature the heat transfer coefficient decreases with increasing heat flux.
4. The general effects may be accounted for a two-resistance concept, which considers the thermal conductivity near the wall and heat capacity some distance from the wall.

ACKNOWLEDGMENT

The authors would like to acknowledge the interesting discussions about this research with Professor John C. Slattery. The financial support of U.S. Army Research Office (Durham) Contract No. DA-11-022-ORD-2674 for this project is gratefully acknowledged.

NOTATION

C_p = isobaric specific heat, B.t.u./(lb.) (°F.)
h = heat transfer coefficient, B.t.u./(hr.) (sq. ft.) (°F.), h' designates local or point value of h
k = thermal conductivity, B.t.u./(hr.) (ft.) (°F.), k'_w designates average value of k in fluid near the tube wall
N_{Gr} = Grashof number for natural convection
p = pressure, lb./sq. in. abs.
q = heat transfer rate per unit area, B.t.u./(hr.) (sq. ft.)
r = radial distance from axis of tube, ft.
r^+ = dimensionless radius given by

$$R\left(\frac{\tau}{\rho}\right)^{1/2}\left(\frac{\rho}{\mu}\right)_w$$

R = tube radius, ft.
Re = Reynolds number, $2\,Rv\,\rho/\mu$, Re_w and Re designate Reynolds numbers with properties evaluated at the wall and bulk mean temperatures, respectively
t = temperature, °F.
v = velocity, ft./sec.
y = radial distance from tube wall, ft.

Greek Letters

β = dimensionless heat flux parameter given by

$$\frac{q_w\left(\frac{\tau}{\rho}\right)^{1/2}_w}{C_{pw}\,\tau_w\,t_w}$$

μ = viscosity, lb./(hr.) (ft.)
ρ = density, lb./(cu. ft.)
τ = shear stress, lb./(hr.)^2 (ft.)

Subscripts

b = bulk mean condition
c = critical condition
c' = transposed critical condition
o = condition at tube axis
w = condition at tube wall (inside surface)

LITERATURE CITED

1. Abbrecht, P. H., and S. W. Churchill, *A.I.Ch.E. Journal*, **6**, 268 (1960).
2. Bringer, R. P., and J. M. Smith, *ibid.*, **3**, 49 (1957).
3. Deissler, R. G., *Natl. Advisory Comm. Aeronaut. Tech. Note 3016* (1953).
4. ———, *Trans. Am. Soc. Mech. Engrs.*, **76**, 73 (1954).
5. ———, and M. F. Taylor, *Natl. Advisory Comm. Aeronaut. Res. Mem. E 53 B 17* (1953).
6. Del Bene, J. V., and J. P. Barger *Tech. Rept. No. 2, ONR, Contract NONR 1841-(14)*, Mass. Inst. Technol., Cambridge, Massachusetts (1959).
7. Dickinson, N. L., and C. P. Welch, *Trans. Am. Soc. Mech. Engrs.*, **80**, 746 (1958).
8. Goldmann, Kurt, *Chem. Eng. Progr. Symposium Ser. No. 11*, **50**, 105 (1954).
9. Guildner, L. A., *Proc. Natl. Acad. Sci.*, **44**, 1149 (1958).
10. Hartnett, J. P., *Trans. Am. Soc. Mech. Engrs.*, **77**, 1211 (1955).
11. Hendricks, R. C., R. W. Graham, Y. Y. Hsu, and Medeiros, paper presented at Conference of American Rocket Society, Palm Beach, Florida (April, 1961).
12. Hsu, Yih-Yun, and J. M. Smith, *J. Heat Transfer*, **83**, 176 (1961).
13. Jenkin, C. F., *Proc. Roy. Soc. London*, **A98**, 170 (1920).
14. Koppel, L. B., Ph.D. thesis, Northwestern University, Evanston, Illinois (August, 1960); International Developments in Heat Transfer, Am. Soc. Mech. Engrs., Section III, Paper No. 69, p. 579 (1961).
15. ———, and J. M. Smith, *J. Chem. Eng. Data*, **5**, 437 (1960).
16. Knudsen, J. G., and D. L. Katz, "Fluid Dynamics and Heat Transfer," McGraw-Hill, New York (1958).
17. Michels, A., B. Blaisse, and C. Michels, *Proc. Roy. Soc. London*, **A153**, 2-1 (1935).
18. *Ibid.*, **A160**, 358 (1937).
19. Naldrett, S. N., and O. Maass, *Can. J. Research*, **18B**, 322 (1940).
20. Quinn, E. L., and C. L. Jones, "Carbon Dioxide," Reinhold, New York (1936).
21. Sengers, J. V., and A. Michels, "Progress in International Research on Thermodynamic and Transport Properties," p. 434, Academic Press, New York (1962).
22. Wood, R. D., Ph.D. thesis, Northwestern University, Evanston, Illinois (June, 1963).

Manuscript received May 14, 1963; revision received August 5, 1963; paper accepted August 7, 1963.